Microchimica Acta (2022) 189: 292
https://doi.org/10.1007/s00604-022-05396-1

ORIGINAL PAPER

Determination of chlorothalonil levels through inhibitory effect on papain activity at protein-decorated liquid crystal interfaces

Duong Song Thai Duong[1] · Chang-Hyun Jang[1]

Received: 17 March 2022 / Accepted: 22 June 2022 / Published online: 26 July 2022

Abstract

A liquid crystal (LC)-based assay was developed to detect chlorothalonil (CHL). The detection principle is based on (i) the electrostatic interaction between the positively charged protein protamine (PRO) with the negatively charged phospholipid dioleoyl-sn-glycero-3-phospho-rac-(1-glycerol) sodium salt (DOPG) and (ii) the CHL-mediated inhibition of papain (PAP) activity. The aqueous/LC interface was decorated with a monolayer of DOPG and PRO that self-assembled via electrostatic interactions. PAP can hydrolyze PRO, resulting in the realignment of an LC by DOPG, inducing a shift in the LC response from bright to dark. The addition of CHL can inhibit the activity of PAP, leading to the attraction of PRO to DOPG and the consequent disruption of the LC orientation. The orientation change of the LC in the presence or absence of CHL can be observed from the changes in its optical appearance using a polarized light microscope. Under optimal conditions, the developed assay achieved a detection limit of 0.196 pg mL^{-1} within a range of determination of 0.65–200 pg mL^{-1}. The selectivity of the assay was verified in the presence of carbendazim and imidacloprid. The practical application of the proposed assay was demonstrated by its use to determine the levels of CHL in food extracts and environmental samples, which yielded recoveries and relative standard deviations (RSD) in the ranges of 87.39–99.663% and 1.03–6.32%, respectively.

Keywords Liquid crystal · 5CB · Chlorothalonil · Enzymatic reaction · Papain · Protamine · Colorimetry · Polarized light microscopy

Introduction

Chlorothalonil (CHL; 2,4,5,6-tetrachloroisophthalonitrile) is a highly potent, hazardous, non-absorbable, broad-spectrum organochlorine fungicide that is widely used to control disease-carrying insect pests in many crops such as vegetables, fruit trees, rice, and wheat [1, 2]. It is the active ingredient in the fungicide Bravo, which plays a key role in treating barley exposed to the fungus *Ramularia*, which is now recognized as an economically important disease-causing fungus across Europe, Argentina, and New Zealand. However, CHL not only causes poisoning in humans, but is also toxic to fish and aquatic invertebrates. It is relatively stable in the environment and adheres well to plants, resulting in significant amounts of chemical residue in the soil, water, and plants. Thus, CHL poses a significant threat to the environment and human health [3]. Furthermore, CHL was found to exert a carcinogenic effect on rat kidneys and a mutagenic effect on their offspring [4]. This is corroborated by an earlier report from the World Health Organization (WHO), which states that the substance may be toxic to fish and aquatic invertebrates." They also highlighted that exposure to CHL can cause damage to the kidney and stomach and may even cause tumors in rodents. Therefore, WHO classified CHL as a Class 2B carcinogen [5, 6]. Moreover, Canada has adopted specific regulations for CHL levels in freshwater (0.18 μg L^{-1}) [7], while the United Kingdom (UK) and the European Commission have banned the use of CHL in the environment due to its high toxicity even at low doses [8–10]. To date, many strategies for CHL detection have been published, including chromatographic, enzyme-linked immunosorbent assays (ELISAs), fluorescence, colorimetric, chemiluminescence, and terahertz (THz) methods [11–14]. While these techniques are highly selective and sensitive, many require a complex operation, long operation times, cumbersome sample preparation, and complex instruments, limiting their widespread applications. Thus, it is important to develop a convenient and rapid

✉ Chang-Hyun Jang
chjang4u@gachon.ac.kr

[1] Department of Chemistry, Gachon University, San 65, Bokjeong-Dong, Sujeong-Gu, Seongnam-City, Gyeonggi-Do 461-701, South Korea

method to improve the analytical performance of CHL detection in biological applications.

Liquid crystals (LCs) possess many unique liquid–solid properties, such as a sensitive orientation behavior, elastic strain, and birefringence. The long-range orientation order of LCs can convert and amplify chemical and physical events at the interface between water and LCs into optical signals that can be easily observed using a microscope [15–20]. Remarkably, Yang and colleagues have recently developed a LC -based diagnostic kit for naked-eye detection of SARS-CoV2-ssRNA [21]. The authors developed a simple polarized system with 2 polarizing filters that was combined with a smartphone application. The diagnostic kit can be used for reliable self-testing of SARS-CoV-2 at home without the need for complex equipment or procedures. Thus, the potential applications of liquid crystal-based biosensors expand when optical images can be observed with simple polarizers.

The alignment of LCs at the molecular level is extraordinarily sensitive to small changes at the aqueous/LC interface. When LC molecules are oriented perpendicular or parallel to the surface in a homeotropic or planar orientation, biochemical interactions at the aqueous/LC interface can cause LC molecules to transition from a homeotropic to a planar orientation. In real-time assays using LC, the TEM grid is often used to contain the LC, preventing it from moving. The LC layer will have two interfaces: LC/solid surface and aqueous/LC interface. The aqueous/LC interface is often modified or functionalized with DNA, protein, or pH-sensitive molecules. When the system is immersed in the analytical solution, a change in pH or a physical or chemical reaction will result in a change in the orientation of the liquid crystal. [19, 22–24]. As the orientation of LCs rapidly responds to analytes at high sensitivity and spatial resolution, surfactant-laden aqueous/LC interfaces have been widely used in LC-based sensing systems to detect enzymatic activity [20, 25–27] and biomolecular interactions [15, 28, 29]. The major limitation of this method is that it is sensitive to physical influences, such as vibration, temperature, and sound, all of which can affect the arrangement of the LC at the aqueous/LC interface. Sensor systems based on these rely on the orientation transitions of LCs triggered by macromolecular bonds or enzymatic hydrolysis events at these interfaces, which can be easily amplified and converted into optical signals.

Based on the above discussion, we developed a novel LC-based biosensor for the detection of CHL based on the electrostatic interaction between 3-phospho-rac-(1-glycerol) sodium salt (DOPG) and protamine (PRO) in combination with the CHL-mediated inhibition of papain (PAP) activity. The positively charged PRO can strongly attract DOPG electrostatically, thereby disrupting the alignment of LCs. PAP cleaves the C-terminal arginine and lysine residues of PRO, effectively hydrolyzing PRO and disrupting the electrostatic interactions between PRO and DOPG. These events led to DOPG-mediated LC realignment. CHL inhibits PAP activity and reactivates PRO. The change in the alignment of LCs from homeotropic to random results in an optical change from dark to bright. These optical changes form the basis for CHL detection and can be observed under a polarized light microscope (POM). The combination of electrostatic interactions and the inhibitory activity of CHL impart high sensitivity and specificity to a CHL sensing system.

Experimental

Detailed information on the materials and protocol used to treat the surface is provided in the Supporting Information.

Results and discussion

Feasibility of the assay

In this study, an LC-based assay was developed to detect CHL based on the change in the orientation of LCs in response to the electrostatic interaction between DOPG and PRO and the enzymatic reaction between PRO and PAP. According to previous reports [19, 20], PAP activity was inhibited in the presence of CHL. We hypothesized that, in the absence of CHL, PAP hydrolyzes PRO into protein fragments, preventing the electrostatic binding of PRO to the DOPG layer. Thus, the LCs remain in a homeotropic orientation. PAP activity was inhibited in the presence of CHL. Therefore, PRO is absorbed by the DOPG layer, resulting in a disruption in the alignment of the LCs (Fig. 1). This strategy was used to propose an assay design for CHL detection.

To verify the feasibility of CHL detection using our hypothesis, the optical response of LCs was examined after incubation with DOPG and PRO, followed by treatment with PAP and CHL. After decoration with self-assembling monolayers (SAMs) of DOPG at the aqueous/LC interface, the LC displayed a uniform dark optical texture, which is indicative of its homeotropic orientation (Fig. 2a(i)). Analysis of the optical response of the LC revealed a bright optical image (Fig. 2a(ii)) upon reaction with PRO because the highly positively charged PRO could strongly and electrostatically attract DOPG and disrupt the alignment of the LC. After this, PAP was added to the mixture. In the absence of the inhibitory effect of CHL, PAP completely cleaved the C-terminal arginine and lysine residues and effectively hydrolyzed PRO. The LCs were then homeotropically aligned through the alignment of DOPG, resulting in a uniform dark optical image (Fig. 2a(iii)). The presence of CHL inhibited PAP activity and protected PRO from hydrolysis. Thus, the obtained optical image was bright (Fig. 2a(iv)). These results confirmed the feasibility of an LC-based assay for CHL detection.

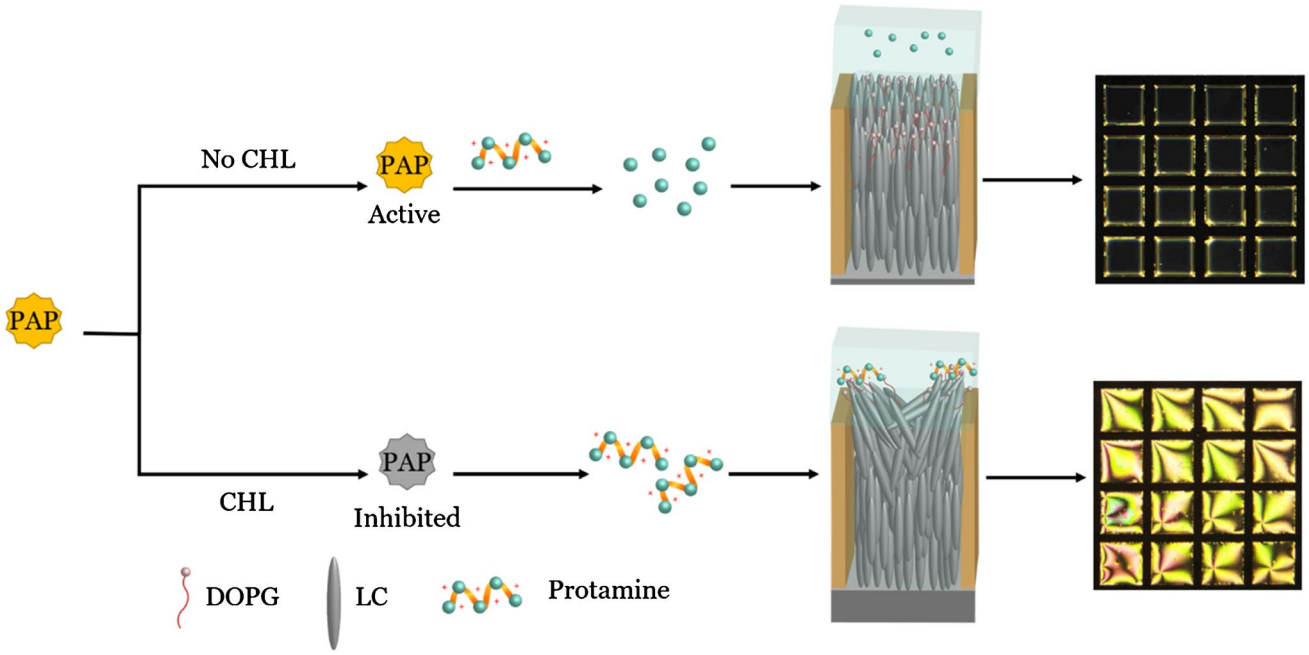

Fig. 1 Schematic diagram of the principle of the LC-based assay for CHL detection

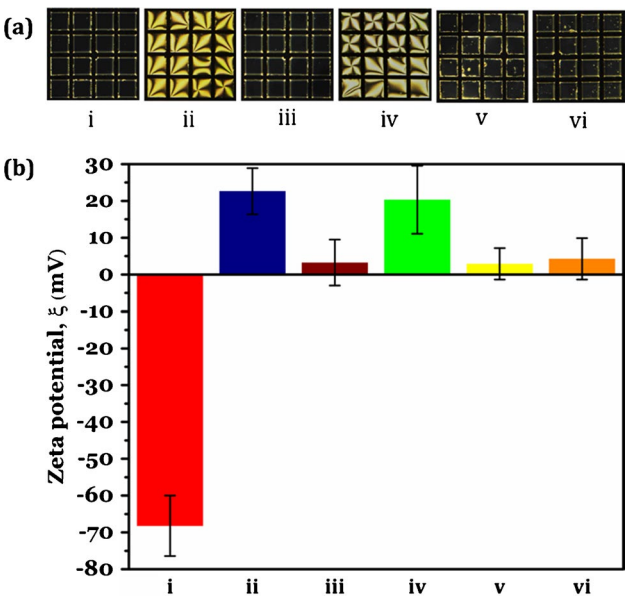

Fig. 2 (**a**) Optical response of the LCs supported on OTS glass slides after decoration of the aqueous/LC interface with (i) 100 μM DOPG, followed by incubation with (ii) 200 μg mL^{-1} PRO, followed by the addition of (iii) 100 μg mL^{-1} PAP, (iv) 100 μg mL^{-1} PAP + 10 ng mL^{-1} CHL, (v) 100 μg mL^{-1} PAP + 10 ng mL^{-1} carbendazim, or (vi) 100 μg mL^{-1} PAP + 10 ng mL^{-1} imidacloprid. The size of each grid hole is 285 μm. (**b**) The zeta potentials of (i) DOPG, (ii) PRO, and solutions containing (iii) PRO and PAP; (iv) PAP, CHL, and PRO; (v) PAP, carbendazim, and PRO; and (vi) PAP, imidacloprid, and PRO

Next, we analyzed the zeta potentials of PRO and DOPG to confirm their interaction in the absence and presence of CHL. The zeta potentials of DOPG and PRO were − 68.2 and 22.62 mV, respectively (Fig. 2b(i-ii)), which confirmed the electrostatic attraction between them at the aqueous/LC interface, disrupting the orientation of the LCs. When PRO was incubated with PAP, the zeta potential decreased to 3.25 mV, owing to the release of free amino acids during PRO hydrolysis (Fig. 2b(iii)). The zeta potential after the introduction of CHL was 20.32 mV, which was similar to the original zeta potential of PRO. Remarkably, no significant change was observed when CHL was replaced with carbendazim or imidacloprid, which are broad-spectrum fungicides (Fig. 2b(iv-vi)). These results suggested that CHL could effectively inhibit PAP.

To further confirm the specificity of the inhibition of PAP activity by CHL, we replaced CHL with 100 μg mL^{-1} carbendazim and imidacloprid. The optical image obtained did not change significantly compared to that obtained in the absence of CHL. This finding indicated that these common interfering substances did not significantly inhibit the enzymatic activity of PAP. Combined with the optical results, this finding demonstrated that our biosensor exhibited good specificity for CHL detection.

However, when the assay was applied to samples spiked with metals (assuming that the samples were contaminated with metals), there was a significant increase in the optical intensity when the metal concentration was higher than 1 nM (10 and 50 nM) (Fig. 3). This limitation was due to the decoration of the negatively charged DOPG layer at the aqueous/

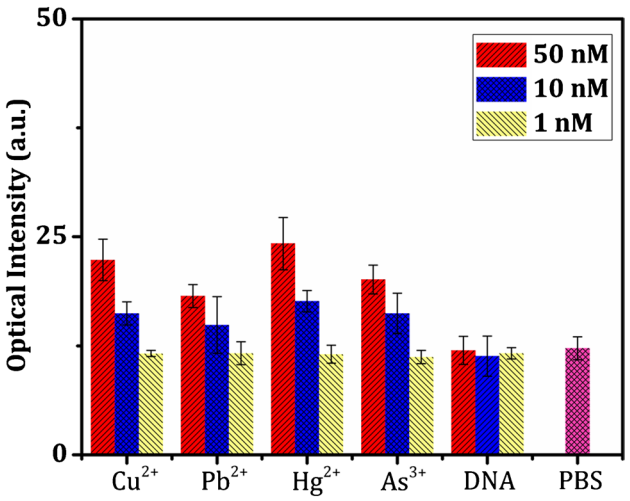

Fig. 3 Optical intensity measurements obtained after 30 min of incubation with a solution containing 100 μg mL^{-1} PAP and three concentrations (1, 10, 50 nM) of metal ions and DNA. PBS was used as a control

LC interface. At high concentrations, the positively charged metal ions interacted with DOPG, interfered with the alignment of the LCs, and led to an increase in the optical intensity, and thus a false-positive result. In contrast, there was no significant change in the optical intensity when a solution spiked with 1 nM metal ions was introduced compared to PBS. When a DNA solution (containing random 50-mers) was applied, the optical intensity did not change because of the similar charges of DNA and DOPG (Fig. 3).

Optimization of the basic condition

Results and discussion regarding the optimization of basic conditions are provided in section S2 of the Supporting Information.

Monitoring the hydrolytic activity of PAP with PRO

PAP is a sulfhydryl hydrolase containing the catalytic triad Cys25, His159, and Asn158 in its active central sites [5]. PAP activity can be inhibited by thiol proteinase inhibitors (E-64), cysteine proteinases, or protease inhibitors. Enze et al. investigated the mechanism of the CHL-induced inhibition of PAP activity by analyzing the fluorescence spectra, Fourier transform infrared spectroscopy (FTIR), and circular dichroism (CD) spectra. The results showed that CHL could interact with certain groups of PAP, leading to changes or inhibition of chemical synthesis, which in turn results in changes in the vibration at the bands and conformation of PAP, and affects its activity [12]. The authors also pointed out that the presence of common pesticides did not significantly affect the PAP assay, which can be explained by the fact that many of them are organophosphates or carbamates. They inhibit acetylcholinesterase (AChE) activity by phosphorylating or carbamoylating the nucleophilic serine residue at the active site.

PAP can hydrolyze PRO by completely cleaving its C-terminal arginine and lysine residues, thereby disrupting the electrostatic interaction between PRO and DOPG. Hence, we assumed that a bright-to-dark shift in the optical response

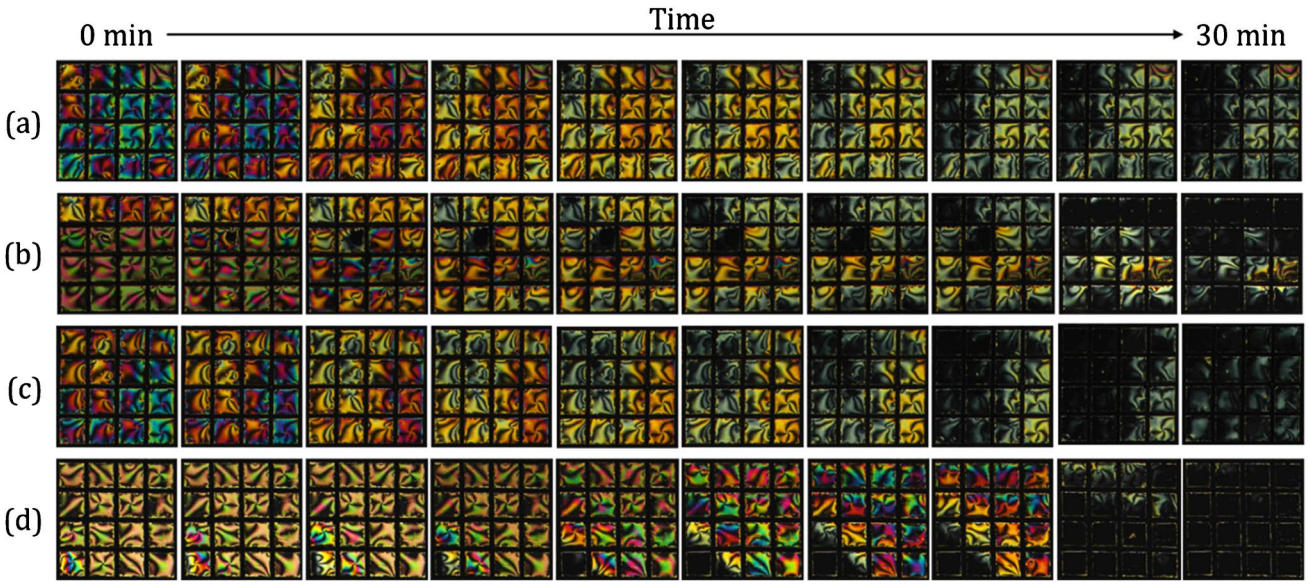

Fig. 4 Optical images of the LCs observed under a POM after decorating the surface with 200 nM DOPG and 115 μg mL^{-1} PRO, then incubation with PAP at concentrations of (**a**) 10 ng mL^{-1}, (**b**) 15 ng mL^{-1}, (**c**) 20 ng mL^{-1}, and (**d**) 25 ng mL^{-1} for 30 min. The size of each grid hole is 285 μm

of LCs would occur after adding an aqueous PAP solution to a PRO-decorated LC interface. First, 200 µL of an aqueous solution containing 10 ng mL^{-1} PAP in PBS was added to the PRO-decorated LC interface. The optical appearance of the solution gradually darkened. However, after 30 min of incubation, the optical images obtained exhibited an incompletely dark appearance (Fig. 4a). This observation indicates that 10 ng mL^{-1} PAP was insufficient to fully hydrolyze PRO, resulting in a disturbance in the LC orientation. The resulting optical images were still partially bright when the PAP concentration was increased to 15 and 20 ng mL^{-1} (Fig. 4b–c). When 25 ng mL^{-1} PAP was added, the optical response of the LC was completely dark (Fig. 4d). This result implies that the PRO decorated at the interface was fully hydrolyzed, which restored the homeotropic orientation of the LCs. These observations prove that the enzymatic reactions involving PAP and PRO can be monitored through the interaction between the positively charged PRO and negatively charged DOPG at the aqueous/LC interface.

CHL detection limit of the LC-based assay

CHL inhibits PAP activity; it interacts with certain PAP groups and changes the vibrations of the bands and PAP conformation, thus limiting its enzymatic activity [5]. Under optimal conditions, the DOPG/PRO and PAP systems were used to detect CHL. The intensity of the optical images changed upon incubation with different concentrations of CHL (Fig. 5a). Over time, the observed optical images revealed significant differences in the output signals when 10 ng mL^{-1} and 0.1 pg mL^{-1} CHL were added. Specifically, there was no significant change in the obtained optical

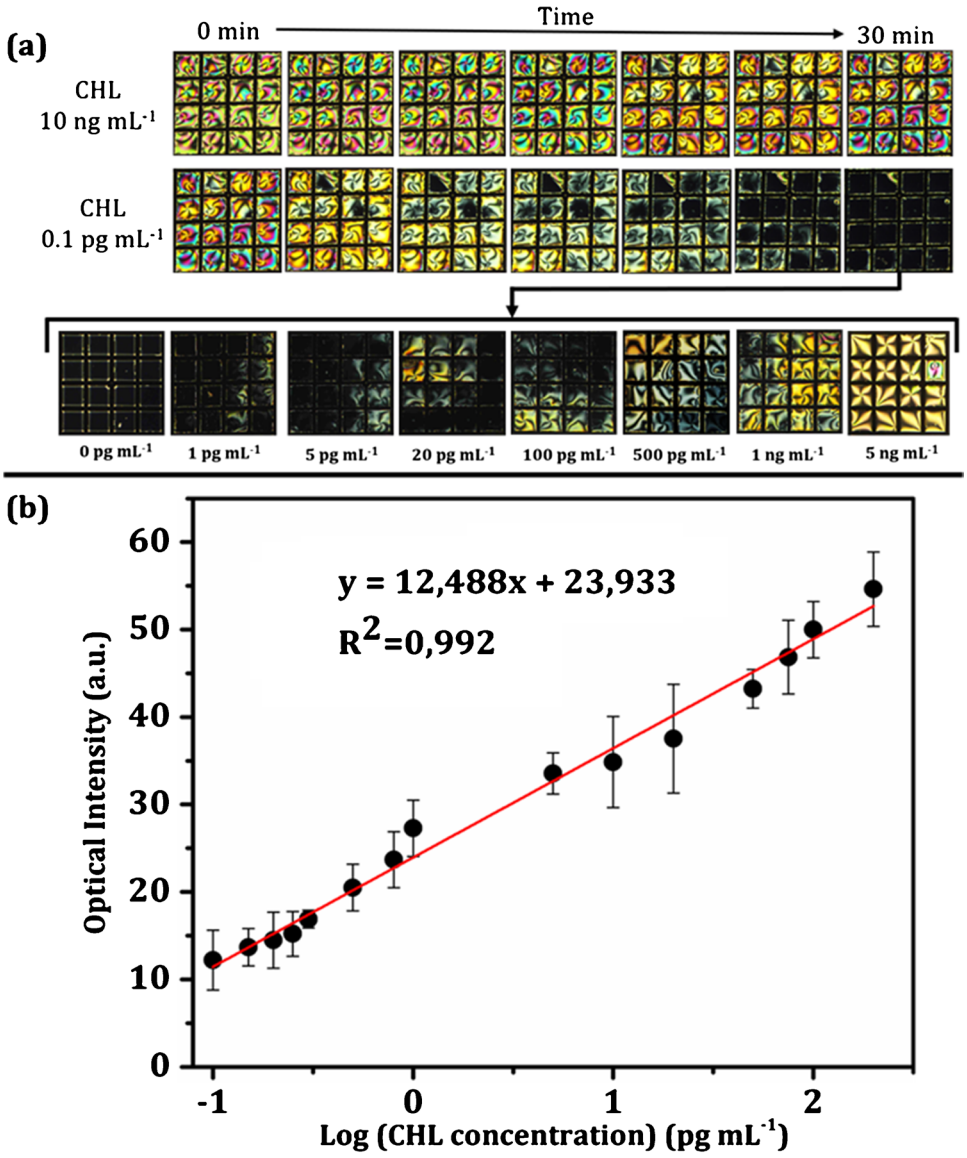

Fig. 5 (**a**) Optical images of the LC interface decorated with DOPG/PRO after incubation with a solution containing 25 ng mL^{-1} PAP and different concentrations of CHL for 30 min. The size of each grid hole is 285 µm. (**b**) Plot showing the linear correlation between the logarithmic CHL concentration and the obtained optical intensity in the range of 0.2–200 pg mL^{-1}

Table 1 Comparison of the proposed method with other methods currently used for CHL detection

Method	Material	LOD (ng mL^{-1})	Detection range (ng mL^{-1})	Ref
Colorimetric	Ultrathin MnO_2 nanosheets	0.024	0.45–3,430	[5]
Colorimetric	The inhibition of GAPDH activity by CHL	0.050 μM	0.5–10 μM	[30]
Colorimetric	Citrate-capped gold nanoparticles	3.6	5.0–100.0	[31]
Fluorometric	Ratiometric fluorescent quantum dot	0.0017	0.34–2,320	[12]
Terahertz metasensor	The four-split ring resonators	1000		[32]
SPR	A monoclonal antibody to CHL, TPN9A		8.0–44.0	[13]
Liquid crystal	Inhibition of papain activity by CHL	0.000196	0.00065–0.2	This study

images after incubation with 10 ng mL^{-1} CHL, while the LC became darker after incubation with 0.1 pg mL^{-1} CHL, which appeared uniformly dark within 30 min. The bright area of the copper grid was proportional to the CHL concentration. In the control experiment, in which CHL was replaced by PBS, the optical image showed a uniform dark appearance. At a CHL concentration of 1 pg mL^{-1}, the LCs appeared as several small bright spots. When the CHL concentration was increased to 5 ng mL^{-1}, the optical image was completely bright. Beyond this value, the intensity of the optical image was saturated. Thus, increasing the CHL concentration did not cause a significant difference in the intensity of the optical image.

ImageJ software was used to record the optical intensities of the obtained images. Figure 5b shows a plot illustrating the correlation between the logarithmic CHL concentration and optical intensity. CHL was examined in the concentration range of 0.1 pg mL^{-1} to 200 pg mL^{-1}. The limit of detection (LOD) and limit of quantification (LOQ) was calculated using the following equations: $LOD = 3\sigma/m$; $LOQ = 10\sigma/m$; (where σ is the standard deviation of the blank or standard deviation of the intercept and m is the slope of the calibration plot).The assay had a limit of detection of 0.196 pg mL^{-1} in the detection range of 0.65–200 pg mL^{-1}. Owing to the sensitivity of the LCs toward the chemical reaction at the aqueous/LC interface, the LOD of the proposed assay was lower than that of the sensors reported in previous studies (Table 1). The response time for this method was approximately 90 min, which was more robust than most existing analytical methods. Therefore, this sensing system is a rapid and reliable method for detecting CHL.

The potential practicability of this assay was evaluated by using it to determine various amounts of CHL spiked in real samples, such as food extracts (apple, pear, grape, orange, and cucumber), tap water, and soil. Before being spiked with CHL, the obtained samples were tested using the proposed assay. The results showed that all the samples contained CHL levels below the LOD of the assay. Predetermined amounts of CHL (10, 500, and 10,000 pg mL^{-1}) were then added to the spiked samples. The samples were then filtered and diluted tenfold to minimize the matrix effect. Measurements were performed according to the protocol presented in Section S1.8, and the results are presented in Table 2. Accordingly, the proposed assay yielded recoveries and relative standard deviations (RSD) in the ranges of 87.39–99.66% and 1.03–6.32%, respectively. In addition, this method met the requirements of the guidelines for pesticide residues in China (NY/T 788–2018). These

Table 2 Amount of chlorothalonil (CHL) detected by the proposed assay versus the actual spiked concentration. The ratio between the detected concentration and the spiked concentration was reported as the mean recovery

Sample	CHL		
	Spiked concentration (pg mL^{-1})	Detected concentration (pg mL^{-1})	Mean recovery ± RSD (%, n = 3)
Apple	1	0.89	89.20 ± 3.26
	50	46.61	93.22 ± 2.36
	1000	966.23	99.62 ± 1.36
Pear	1	0.95	95.20 ± 2.12
	50	47.34	94.68 ± 6.32
	1000	953.26	95.32 ± 1.29
Grape	1	0.89	89.70 ± 1.95
	50	45.24	90.49 ± 2.97
	1000	954.78	95.47 ± 1.03
Orange	1	0.98	98.20 ± 3.69
	50	46.68	93.37 ± 5.63
	1000	963.16	96.31 ± 1.06
Cucumber	1	0.99	99.80 ± 3.06
	50	43.70	87.39 ± 4.26
	1000	976.65	97.66 ± 2.87
Tap water	1	0.94	93.60 ± 1.15
	50	49.24	98.47 ± 2.93
	1000	964.33	96.43 ± 4.23
Soil	1	0.96	95.80 ± 1.38
	50	45.70	91.39 ± 4.06
	1000	996.63	99.66 ± 6.06

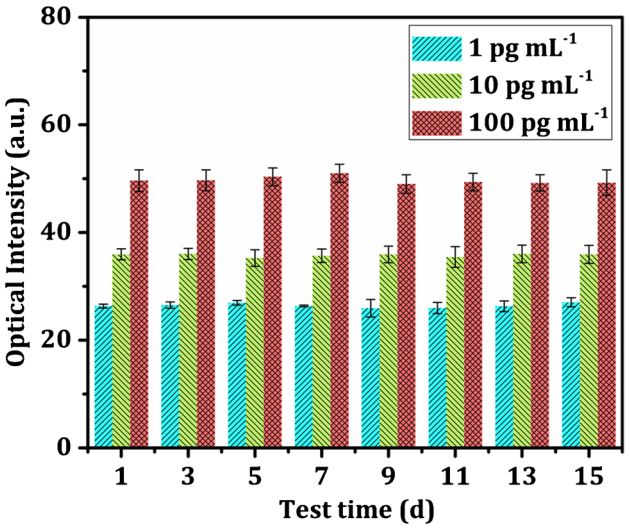

Fig. 6 Stability of the assay. Three CHL concentrations (1, 10, 100 pg mL^{-1}) were added to the detection platform and optical intensity was monitored for 15 days

findings confirmed the precision and reproducibility of the developed assay for quantifying CHL levels in food and environmental samples.

Stability of the assay

To investigate the stability of the assay, CHL at three concentrations (1, 10, 100 pg mL^{-1}) was introduced to the detection platform and incubated. The optical response of the LCs was observed for 15 d, and the results are shown in Fig. 6. At the end of the observation period, the three CHL concentrations showed similar responses, respectively, to those on the first day. Thus, the proposed assay was stable.

Conclusion

In conclusion, an assay based on LC was developed in this study to monitor CHL levels by inhibiting the activity of PAP via the electrostatic interaction between DOPG and PRO. PAP hydrolyzes PRO in the absence of CHL, disrupting the electrostatic interactions between the negatively charged DOPG and the positively charged PRO. The homeotropic orientation of the LCs was maintained. The presence of CHL inhibited PAP and prevented the hydrolysis of PRO. Thus, the alignment of LC was disrupted when PRO was electrostatically attracted to the DOPG layer, resulting in a change in the optical response of LC from dark to bright. Introduction of a mixed solution of PAP and carbendazim or imidacloprid did not result in significant optical changes, demonstrating the high selectivity of CHL over PAP. The assay had higher sensitivity and specificity, wider linear range and a faster response than conventional detection methods. The assay also showed high accuracy and reliability in detecting CHL in real samples. The stability tests that the proposed assay exhibited good stability.

Supplementary Information The online version contains supplementary material available at https://doi.org/10.1007/s00604-022-05396-1.

Acknowledgements This study was supported by the Basic Science Research Program of the National Research Foundation of Korea (NRF), funded by the Ministry of Education [NRF- 2019R1A2C1003862].

Declarations

Conflict of interest The authors report no potential conflict of interest.

References

1. Simões T, Novais SC, Natal-da-Luz T, Leston S, Rosa J, Ramos F et al (2019) Fate and effects of two pesticide formulations in the invertebrate Folsomia candida using a natural agricultural soil. Sci Total Environ 675:90–97
2. Xu X-H, Liu X-M, Zhang L, Mu Y, Zhu X-Y, Fang J-Y et al (2018) Bioaugmentation of chlorothalonil-contaminated soil with hydrolytically or reductively dehalogenating strain and its effect on soil microbial community. J Hazard Mater 351:240–249
3. Yu H, Xu L, Yang F, Xie Y, Guo Y, Cheng Y et al (2021) Rapid Surface-Enhanced Raman Spectroscopy Detection of Chlorothalonil in Standard Solution and Orange Peels with Pretreatment of Ultraviolet Irradiation. Bull Environ Contam Toxicol 107:221–227
4. da Silveira Guerreiro A, Rola RC, Rovani MT, da Costa SR, Sandrini JZ (2017) Antifouling biocides: impairment of bivalve immune system by chlorothalonil. Aquat Toxicol 189:194–199
5. Sheng E, Lu Y, Tan Y, Xiao Y, Li Z, Dai Z (2020) Oxidase-mimicking activity of ultrathin MnO2 nanosheets in a colorimetric assay of chlorothalonil in food samples. Food Chem 331:127090
6. W.H. Organization (2020) WHO recommended classification of pesticides by hazard and guidelines to classification, 2019 edition.
7. Marine N (1999) Canadian water quality guidelines for the protection of aquatic life. Canadian Council of Ministers of the Environment, Winnipeg, pp 1–5
8. E.F.S. Authority, Arena M, Auteri D, Barmaz S, Bellisai G, Brancato A et al (2018) Peer review of the pesticide risk assessment of the active substance chlorothalonil. EFSA J 16:05126
9. Lopes FC, Junior ASV, Corcini CD, Sánchez JAA, Pires DM, Pereira JR et al (2020) Impacts of the biocide chlorothalonil on biomarkers of oxidative stress, genotoxicity, and sperm quality in guppy Poecilia vivipara. Ecotoxicol Environ Saf 188:109847
10. E. Commission (2019) Draft Commission Implementing Regulation concerning the non-renewal of the approval of the active substance chlorothalonil, in accordance with Regulation (EC) No 1107/2009 of the European Parliament and of the Council concerning the placing of plant protection products on the market, and amending Commission Implementing Regulation (EU) No 540/2011
11. Kurz MH, Gonçalves FF, Adaime MB, da Costa IF, Primel EG, Zanella R (2008) A gas chromatographic method for the determination of the fungicide chlorothalonil in tomatoes and cucumbers

and its application to dissipation studies in experimental greenhouses. J Braz Chem Soc 19:1129–1135
12. Sheng E, Lu Y, Tan Y, Xiao Y, Li Z, Dai Z (2020) Ratiometric fluorescent quantum dot-based biosensor for chlorothalonil detection via an inner-filter effect. Anal Chem 92:4364–4370
13. Hirakawa Y, Yamasaki T, Watanabe E, Okazaki F, Murakami-Yamaguchi Y, Oda M et al (2015) Development of an immunosensor for determination of the fungicide chlorothalonil in vegetables, using surface plasmon resonance. J Agric Food Chem 63:6325–6330
14. da Silva RJB, Dias PM, Camões MFG (2012) Development and validation of a grouping method for pesticides analysed in foodstuffs. Food Chem 134:2291–2302
15. Brake JM, Daschner MK, Luk Y-Y, Abbott NL (2003) Biomolecular interactions at phospholipid-decorated surfaces of liquid crystals. Science 302:2094–2097
16. Lowe AM, Ozer BH, Bai Y, Bertics PJ, Abbott NL (2010) Design of surfaces for liquid crystal-based bioanalytical assays. ACS Appl Mater Interfaces 2:722–731
17. Yin F, Cheng S, Liu S, Ma C, Wang L, Zhao R et al (2021) A portable digital optical kanamycin sensor developed by surface-anchored liquid crystal droplets. J Hazard Mater 420:126601
18. Hong PTK, Yun K, Jang C-H (2021) Liquid crystal-based droplet sensor for the detection of Hg (II) ions using an aptamer as the recognition element. BioChip J 15:152–161
19. Duong TDS, Jang C-H (2021) Detection of arginase through the optical behaviour of liquid crystals due to the pH-dependent adsorption of stearic acid at the aqueous/liquid crystal interface. Sens Actuators B Chem 339:129906
20. Hu Q-Z, Jang C-H (2012) Imaging trypsin activity through changes in the orientation of liquid crystals coupled to the interactions between a polyelectrolyte and a phospholipid layer. ACS Appl Mater Interfaces 4:1791–1795
21. Xu Y, Rather AM, Song S, Fang J-C, Dupont RL, Kara UI et al (2020) Ultrasensitive and selective detection of SARS-CoV-2 using thermotropic liquid crystals and image-based machine learning. 1:100276
22. Kim C, Jang C-H (2021) Liquid crystal-based aptasensor to detect ractopamine hydrochloride at a femtomolar level. Microchem J 171:106861
23. Nguyen DK, Jang C-H (2021) A cationic surfactant-decorated liquid crystal-based aptasensor for label-free detection of malathion pesticides in environmental samples. Biosensors 11:92
24. Khan M, Khan AR, Shin J-H, Park S-Y (2016) A liquid-crystal-based DNA biosensor for pathogen detection. Sci Rep 6:1–12
25. Nguyen DK, Jang C-H (2020) Label-free liquid crystal-based detection of As (III) ions using ssDNA as a recognition probe. Microchem J 156:104834
26. Liu D, Jang C-H (2014) A new strategy for imaging urease activity using liquid crystal droplet patterns formed on solid surfaces. Sens Actuators B Chem 193:770–773
27. Wang Y, Hu Q, Guo Y, Yu L (2015) A cationic surfactant-decorated liquid crystal sensing platform for simple and sensitive detection of acetylcholinesterase and its inhibitor. Biosens Bioelectron 72:25–30
28. McUmber AC, Noonan PS, Schwartz DKJSM (2012) Surfactant–DNA interactions at the liquid crystal–aqueous interface. Soft Matter 8:4335–4342
29. Price AD, Schwartz DK (2008) DNA hybridization-induced reorientation of liquid crystal anchoring at the nematic liquid crystal/aqueous interface. J Am Chem Soc 130:8188–8194
30. Liu Q, Han P, Wang H, Gong W, Feng X (2019) Antibody-free colorimetric detection of chlorothalonil in cucumber via the inhibition of an enzyme-triggered reaction. RSC Adv 9:9893–9898
31. Liu Q, Han P, Gong W, Wang H, Feng X (2018) Colorimetric determination of the pesticide chlorothalonil based on the aggregation of gold nanoparticles. Microchim Acta 185:1–7
32. Zhang Y, Ye Y, Song X, Yang M, Ren Y, Ren X et al (2020) High-sensitivity detection of chlorothalonil via terahertz metasensor. Mater Res Express 7:095801